

**Anomalous enhancement in magnetization on interstitial doping due to spin reversal in magnetic materials**

**Nidhi Singh\*, Kritika Anand, Nithya Christopher, Amrita Bhattacharya, A. K. Srivastava**

CSIR-National Physical Laboratory, and Academy of Scientific & Innovative Research (AcSIR),  
Dr. K. S. Krishnan Road, New Delhi 110 012, India

\*Corresponding author's email: [singhnidhi@nplindia.org](mailto:singhnidhi@nplindia.org)

Phone No.: +91-11- 4560 9455/8559, Fax no. : +91-11- 4560 9310

### X-ray diffraction of the synthesized samples:

The XRD patterns of pristine  $\text{Mn}_2\text{Sb}$  and Boron doped  $\text{Mn}_2\text{Sb}$  with optimized Boron concentrations and optimally annealed protocols are shown in Fig. S1 (a). The figure suggests that the pristine  $\text{Mn}_2\text{Sb}$  alloy was indexed for single phase  $\text{Mn}_2\text{Sb}$  whereas in Boron-doped  $\text{Mn}_2\text{Sb}$  elemental Sb and Mn peaks also exist as a minor phase. Expectedly, the peaks corresponding to  $\text{Mn}_2\text{Sb}$  phase were found to shift towards lower diffraction angles, post Boron doping. This confirms the inclusion of Boron in  $\text{Mn}_2\text{Sb}$  matrix. The Rietveld refinement of  $\text{Mn}_2\text{SbB}$  compound was carried out using FullProf suite (Fig. S1 (b)). It was done to confirm the phase formation as well as to determine the phase fraction of the alloy formed. The  $\text{Cu}_2\text{Sb}$  tetragonal crystal structure is still preserved with lattice parameters  $a = b = 4.079 \text{ \AA}$  and  $c = 6.562 \text{ \AA}$ . Also, the phase fraction of  $\text{Mn}_2\text{SbB}$  was found to be 97.1 % and the rest 2.9 % accounts for the elemental Sb and Mn impurities. Although minor impurity elements are present but Sb in elemental state being diamagnetic and Mn being paramagnetic do not contribute towards the magnetization observed in the present study. Infact these impurities lead to domain wall hindrance, resulting in an increase in coercivity.

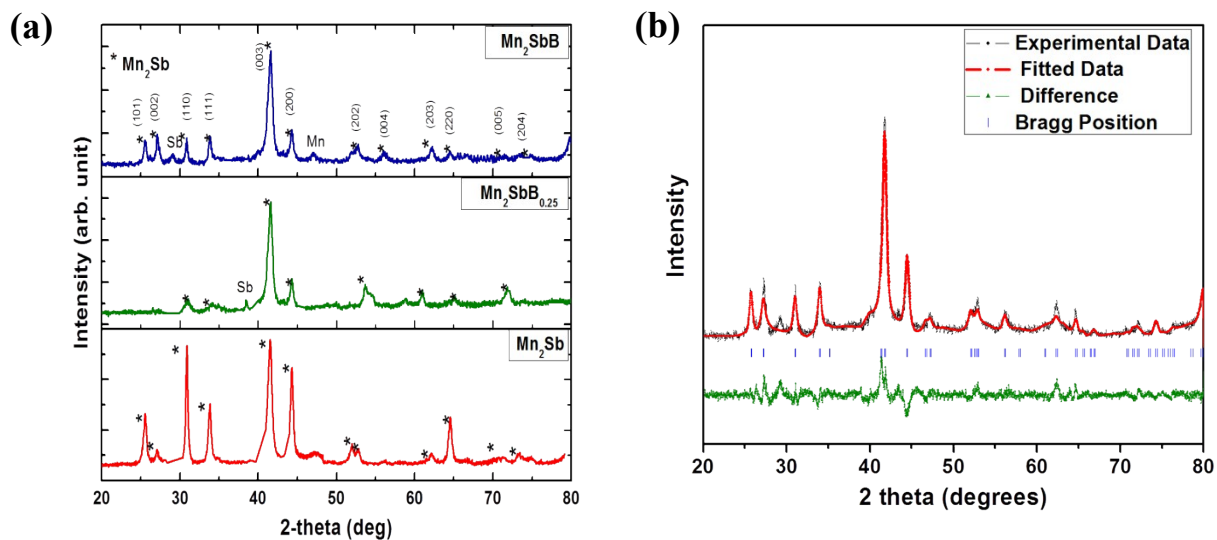


**FIG. S1.** (a) XRD patterns of  $\text{Mn}_2\text{SbB}_n$  alloys synthesized employing arc melting & ball milling followed by annealing. (b) Rietveld refinement of XRD pattern of  $\text{Mn}_2\text{SbB}$ , the bottom line curve shows the difference between the measured and fitted curves, and the vertical line indicates the Bragg position of the  $\text{Mn}_2\text{SbB}$  phase.

### **HRTEM analysis of the synthesized samples:**

A detailed microstructural characterization on synthesized sample of  $\text{Mn}_2\text{SbB}$  elucidated several interesting features in real and reciprocal space. Fig. S2 (a) indicates a uniform microstructure at low magnification. The fine microstructure reveals the grain sizes ranging from about 7 to 11 nm (as marked in Fig. S2 (a)). The fine domains with bright and dark contrast are marked with a set of arrows in upper inset of Fig. S2 (a) which appears to converge at the grain boundaries (encircled in upper inset, Fig. (S2 (a))). At higher magnifications, within the individual domains, thick fringes were revealed due to magnetic anisotropy in the structure of the material. The chemistry of the material was examined employing energy dispersive x-ray spectroscopy (EDXS) attached to the HRTEM and the image recorded on the corresponding region using scanning transmission electron microscopy (STEM) detector is displayed as an inset in Fig. S2 (b). The EDXS intensity profile exhibits the presence of the peaks with energy levels of Boron (0.183 keV;  $\text{K}\alpha_{1,2}$ ), Sb (3.844 keV;  $\text{L}\beta_1$ , 4.101 keV;  $\text{L}\beta_2$ , 4.348 keV;  $\text{L}\gamma_1$ ) and Mn (6.49 keV;  $\text{K}\beta$ , 6.53 keV;  $\text{K}\alpha_{1,2}$ ). The presence of O (0.525 keV;  $\text{K}\alpha_{1,2}$ ) and Cu (8.041 keV;  $\text{K}\alpha_{1,2}$ , 8.905 keV;  $\text{K}\beta$ ) in the spectrum arises due to obvious reasons and may be attributed as expected impurity. Fig. S2 (c) elucidates the occurrence of two well-oriented crystallites with the inter-planar spacing of 0.35 and 0.33 nm corresponding to 101 and 002 planes of  $\text{Mn}_2\text{Sb}$  respectively (space group:  $\text{P4/nmm}$ , lattice parameters:  $a = 0.4098$  nm,  $c = 0.6653$  nm, reference: JCPDS file no. 00-004-0822). The boundary between these two crystals (marked as A and B) is separated by a

white dotted line in Fig. S2 (c). It was noted that the angular separation between these two crystallites was about  $75^\circ$ , which was further authenticated by measuring the angles between these two planes (101 and 002) with the same inter-planar spacing in reciprocal space by recording the corresponding fast Fourier transform (FFT) of the particular atomic-scale image (inset in Fig. S2 (c)). The angular separation of  $75^\circ$  between 101 and 002 planes is also well corroborated with a tetragonal crystal structure of  $\text{Mn}_2\text{Sb}$ . A superimposed region (marked as C in Fig. S2 (c)) of two crystallites noticeably distinguishes the atomic sites of both the set of planes (101 and 002). A region marked as 'D' in Fig. S2 (c) shows a low angle boundary which is decorated with amorphous and crystalline structures, as evident by discontinuous high indices crystallographic planes with very fine interplanar spacing. Fig. S2 (d) exhibits the two sets of planes of  $\text{Mn}_2\text{Sb}$  (hkl: 101, marked as E) and Boron (hkl: 104, interplanar spacing: 0.51 nm, marked as F) abutting each other (encircled with a region denoted as G). An exploration in various regions at an atomic-scale elucidates that the Boron lattice is interpenetrating in the interstitial of  $\text{Mn}_2\text{Sb}$  lattice with the stacking of planes (104) well organized (Fig. S2 (e)). Atomic planes were constituted of  $\text{Mn}_2\text{Sb}$  with the stacking sequence of hkl: 111 (interplanar spacing: 0.26 nm). The coordinates of these two set of planes are such that the overall appearance of the composite microstructure at lattice scale in the image plane (Fig. S2 (e)) seems to be as columnar. A schematic of stacking sequence of Boron (104) and  $\text{Mn}_2\text{Sb}$  (111) planes at lattice site apparently demonstrates the interstitial doping of Boron into  $\text{Mn}_2\text{Sb}$ -lattice.

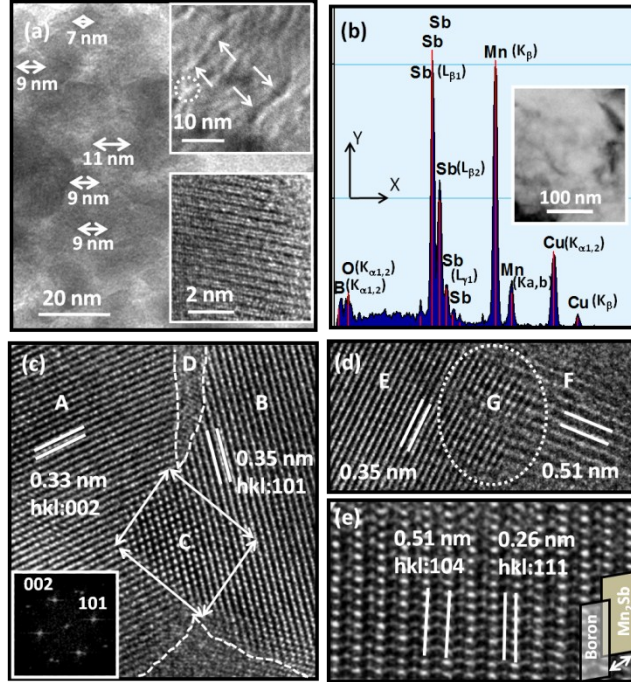


**FIG. S2.** HRTEM images of  $\text{Mn}_2\text{SbB}$ . (a) Uniform fine-grained densely packed microstructure, (b) EDXS pattern with X-axis: Energy (keV), Y-axis: intensity (counts, arb. units), (c) distribution of different crystallites (A and B) with boundaries marked with white dotted lines, region C is a superimposed region of A and B; region D is due to a low angle boundary evolved between crystallites of A and B, (d) regions E and F denotes the atomic planes of  $\text{Mn}_2\text{Sb}$  (101) and Boron (104, interplanar spacing: 0.51 nm), respectively. Region G is evolved due to abutting planes of  $\text{Mn}_2\text{Sb}$  and Boron, and (e) stacking of atomic planes of Boron (104) coexisting with  $\text{Mn}_2\text{Sb}$  (111) planes. **Insets:** (a) upper micrograph is a distribution of domains in the microstructure and convergence domain walls into grain boundaries, lower micrograph is an image of thick fringes evolved within the domains, (b) STEM micrograph, (c) FFT recorded from the regions composite of A, B and C, and (e) schematic showing the arrangement of Boron and  $\text{Mn}_2\text{Sb}$  planes.